Gravitational Microlensing by Globular Clusters

Philippe Jetzer[1,2]**, Marcus Strässle**[2] **and Ursula Wandeler**[2]

[1] Paul Scherrer Institut, Laboratory for Astrophysics, CH-5232 Villigen PSI
[2] Institut für Theoretische Physik der Universität Zürich, Winterthurerstrasse 190, CH-8057 Zürich

Abstract. Stars in globular clusters can act either as sources for MACHOs (Massive Astrophysical Compact Halo Objects) located along the line of sight or as lenses for more distant background stars. Although the expected rate of microlensing events is small, such observations can lead to very useful results. In particular, one could get information on the shape of the galactic halo along different lines of sight, allowing to better constrain its total dark matter content.

Moreover, on can also infer the total dark matter content of globular clusters, which is presently not well known. To this latter purpose, we analyse the microlensing events towards the galactic bulge, which lie close to the three globular clusters NGC 6522, NGC 6528 and NGC 6540. We find evidence that some microlensing events are indeed due to MACHOs located in the globular clusters, suggesting, therefore, that these clusters contain a significant amount of dark matter.

Key words: galactic halo - microlensing - dark matter - globular clusters

1. Introduction

An important problem in astrophysics concerns the nature of the dark matter in galactic halos, whose presence is implied by the observed flat rotation curves in spiral galaxies. Microlensing (Paczyński 1986) allows the detection of MACHOs in the mass range $10^{-7} < M/M_\odot < 1$ (De Rújula, Jetzer, Massó 1992) in the halo, disk or bulge of our galaxy. Till now, more than 15 microlensing events have been found towards the Large Magellanic Cloud (LMC) (Alcock, Akerlof, Allsman et al. 1993, Alcock, Allsman, Alves et al., 1997b, Auburg, Bareyre, Bréhin et al 1993), one event towards the Small Magellanic Cloud (SMC) (Alcock, Allsman, Alves et al. 1997c, Palanque-Delabrouille, Afonso, Albert et al. 1997, Udalski, Kubiak & Szymański

1997) and about 200 events towards the galactic bulge (Alcock, Allsman, Alves et al. 1997a, Udalski, Szymański, Stanek et al. 1994, Alard & Guibert 1997).

However, in spite of the many events, several questions are still open, in particular on the mass and the location of the lenses. In fact, from the duration of a single microlensing event, one cannot infer directly the mass of the lens, since its distance and transverse velocity are generally not known. To break this degeneracy it has been proposed to perform parallax measurements (Gould 1997), which however require the use of space satellites.

Globular clusters could be in many respect very useful to solve some of these problems. In fact, microlensing searches using globular clusters as targets could probe different lines of sight in addition to the ones towards the LMC or the SMC, this way allowing to better determine the spatial distribution of the MACHOs (Jetzer 1991). Since in globular clusters much less stars than compared to the LMC or SMC can be used as targets, one would have to monitor many globular clusters in order to get some microlensing events. Gyuk & Holder (1997) and Rhoads & Malhotra (1997) have studied this possibility and shown that this way interesting galactic structure information can be extracted allowing to distinguish between different halo models.

Another possibility is to search for microlensing of background stars by MACHOs located in foreground globular clusters. Such an observation can in addition give important information on the total mass of globular clusters. It has been argued recently that a large fraction of their mass (around 50%) is dark, which could be in the form of brown dwarfs, low-mass stars or white dwarfs (Heggie et al. 1996, Taillet, Salati & Longaretti 1995, 1996). Moreover, one expects that the heavy stars tend to sink towards the cluster cores, whereas the light objects populate the outskirts. Hence, the dark component of the cluster is not similarly concentrated towards the center as the bright stars which eases observation.

The idea –as originally proposed by Paczyński (1994)– is to monitor globular clusters like 47 Tuc or M22 in front of the rich background of either the SMC or the galactic

bulge. In this case, when the lens belongs to the cluster population, its distance and velocity are roughly known. The velocity is defined by the dispersion velocity of the cluster stars together with the overall transverse velocity of the cluster as a whole. Knowing approximately the distance and the velocity of the lens would allow to extract from a microlensing event the mass of the lens with an accuracy of $\sim 30\%$.

Due to these reasons, it is important to study in more detail microlensing by globular clusters either using their stars as sources, or the dark matter contained in them as lenses for more distant stars (Wandeler 1995). In this paper we discuss both aspects in detail. Although the mass distribution of the luminous part of the cluster, as inferred from the observation of the distribution of the red giant population, agrees well with a King model, we do not consider this to be representative for the population of light objects. Taillet, Longaretti & Salati (1995, 1996) have shown that in an isolated globular cluster thermalisation between the different populations does occur. However, globular clusters –especially the ones towards the bulge– tidally interact with the surrounding material which might counteract thermalisation, hence the consideration of alternative mass distributions should be taken into account and variations of the microlensing event rate due to it might give some hints at the dynamical history of the cluster.

We also analyse the microlensing events towards the galactic bulge, which are close to the three globular clusters NGC 6522, NGC 6528 and NGC 6540. These clusters lie within the observation fields of the MACHO and OGLE teams. We find evidence that some microlensing events are indeed due to MACHOs located in the globular clusters, suggesting therefore that these clusters contain a significant amount of dark matter.

The paper is organized as follows: in Sect. 2 we introduce briefly the basics of microlensing. In Sect. 3 we discuss as an example the globular cluster 47 Tuc, which will then be used to estimate in a very conservative way the optical depth and the lensing rate for other clusters as well. In Sect. 4 we present microlensing using globular clusters towards the galactic bulge. In particular, we analyse the events as reported by the MACHO and the OGLE collaboration lying within a distance of 30 pc around the centers of NGC 6522, NGC 6528 and NGC 6540. In Sect. 5 we conclude with a short summary of our results.

2. Basics of microlensing

For completeness we give here a short summary of the most important formulae of gravitational microlensing; for more details see for instance Jetzer (1997).

The time dependent magnification of a light source due to gravitational microlensing is given by

$$A(t) = \frac{u_\circ^2 + t^2/T_\circ^2 + 2}{\sqrt{(u_\circ^2 + t^2/T_\circ^2)(u_\circ^2 + t^2/T_\circ^2) + 4}}\,, \qquad (1)$$

with $u_\circ = d_{min}/R_E$, where d_{min} is the minimal distance of the MACHO from the line of sight between the source and the observer. R_E is the Einstein radius, defined as

$$R_E^2 = \frac{4GMD}{c^2}x(1-x)\,, \qquad (2)$$

with $x = s/D$, D and s are the distances to the source and the MACHO, respectively. v_T is the relative transverse velocity of the involved objects. $T_\circ = R_E/v_T$ is the characteristic time for the lens to travel the distance R_E.

The probability τ_{opt}, that a source is found within a radius R_E of some MACHO, is defined as

$$\tau_{opt} = \int_0^1 \frac{4\pi G}{c^2}\rho(x)D^2 x(1-x)\,dx\,, \qquad (3)$$

with $\rho(x)$ the mass density of microlensing matter at the distance $s = xD$ from us along the line of sight.

The microlensing event rate is given by (De Rújula, Jetzer, Massó 1991, Griest, Alcock, Axelrod et al. 1991)

$$\Gamma = 2u_{TH}D \int R_E(x)v_T f_T(v_T)\frac{dn}{d\mu}dv_T dx d\mu\,, \qquad (4)$$

where $\mu = M/M_\odot$ and $f_T(v_T)$ is the transverse velocity distribution. The maximal impact parameter u_{TH} is related to the threshold magnification A_{TH} by Eq. (1). In the following we take $A_{TH} = 1.34$ which corresponds to $u_{TH} = 1$. $\frac{dn(x)}{d\mu}$ is the MACHO number density, which for a spherical halo is given by

$$\frac{dn(x)}{d\mu} = \frac{dn_\circ}{d\mu}\frac{a^2 + R_{GC}^2}{a^2 + R_{GC}^2 + D^2x^2 - 2DR_{GC}\cos\alpha}\,, \qquad (5)$$

here α denotes the angle between the line of sight and the direction towards the galactic center. $n_\circ$ is assumed not to depend on x and is normalized such that

$$M_\odot \int \mu\,d\mu\frac{dn_\circ}{d\mu} = \rho_\circ \simeq 7.9 \times 10^{-3}\frac{M_\odot}{\text{pc}^3} \qquad (6)$$

equals the local dark matter mass density. $R_{GC} \simeq 8.5\,\text{kpc}$ is the distance from the Sun to the galactic center and $a \simeq 5.6\,\text{kpc}$ is the core radius of the halo.

For the average lensing duration one gets the following relation

$$\langle T \rangle = \frac{2\tau_{opt}}{\pi\Gamma}u_{TH}\,. \qquad (7)$$

3. The system SMC-47 Tuc: a paradigm for cluster lensing

In this section we thoroughly discuss the basics of microlensing by a globular cluster. We use the system SMC-47 Tuc as an example, but the results, by appropriately scaling them, are valid for other globular clusters as well.

First, we discuss simple models of 47 Tuc which will then be used for the computation of the optical depth and the microlensing event rate for different geometries of lens and source.

The globular cluster 47 Tuc (NGC 104) lies at galactic coordinates $l = 305.9°$, $b = -44.89°$. For the distance we assume 4.1 kpc, although in the literature values up to 4.7 kpc are quoted (Harris 1996). Our choice will rather underestimate the optical depth. The position is such that it overlaps with a part of the outer region of the SMC, which makes it an interesting object. Globular clusters are small objects compared to the scale of their distance, hence they are well suited for gravitational lensing, since one may assume the distance of their stars to be the same for all practical purposes.

3.1. Spatial density and velocity dispersion for 47 Tuc

For the calculation of the lensing rate we need to know the spatial distribution of the dark matter in the globular cluster. Since this is not known, we will instead discuss models for the total mass of the cluster. To get the mass density ρ_d of the dark objects, we then make the simplifying assumption that ρ_d is proportional to the total mass density ρ, i.e. ρ_d is given by

$$\rho_d = f\,\rho = \frac{M_{dark}}{M_{tot}}\rho\,, \qquad (8)$$

where M_{dark} is the total mass of the MACHOs in the cluster. We are aware, that this assumption is oversimplified, however, as long as the content of dark matter in globular clusters is not known, it is one way to parametrize our ignorance. Moreover, since the expected event rate for 47 Tuc is about one event per year or even less, we do not consider multi-mass models for 47 Tuc. We postpone the discussion of them to Sect. 4, when we discuss lensing by globular clusters towards the bulge in which situation the model can be tested due to the higher number of microlensing events.

The simplest model of a globular cluster is a self-gravitating isothermal sphere of identical "particles" (stars). The equilibrium distribution function in phase-space coordinates is

$$f(\boldsymbol{x}, \boldsymbol{v}) = \frac{\rho_\circ}{\left(2\pi \frac{k_B T}{m}\right)^{3/2}}\ \exp\left(\frac{m(\Phi(\boldsymbol{x}) - \frac{1}{2}v^2)}{k_B T}\right)\,, \qquad (9)$$

where $\Phi(\boldsymbol{x})$ is the gravitational potential of the cluster, T the temperature, k_B Boltzmann's constant and m the mass of a "particle". Taking into account the spherical symmetry of the globular cluster and defining the one-dimensional velocity dispersion σ as

$$\sigma = \sqrt{\frac{k_B T}{m}}\,, \qquad (10)$$

Eq. (9) reads

$$f(r, \boldsymbol{v}) = \frac{\rho_\circ}{(2\pi\sigma^2)^{3/2}}\ \exp\left(\frac{\Phi(r) - \frac{1}{2}v^2}{\sigma^2}\right)\,. \qquad (11)$$

Here r is the radial distance relative to the cluster center. Integrating over all velocities, we get

$$\rho(r) = \rho_\circ \exp\left(\frac{\Phi(r)}{\sigma^2}\right)\,. \qquad (12)$$

Inserting Eq. (12) into the Poisson equation for the gravitational potential, one obtains

$$\frac{d}{dr}\left(r^2\,\frac{d\ln\rho}{dr}\right) = -\frac{4\pi G}{\sigma^2}r^2\rho\,. \qquad (13)$$

A solution of this equation is

$$\rho(r) = \frac{\sigma^2}{2\pi G r^2}\,. \qquad (14)$$

The mass density given in Eq. (14), together with the integrated velocity distribution Eq. (11), defines the singular isothermal sphere.

To avoid the singularity at the origin we rescale the variables ($\tilde{r} = r/r_c$, $\tilde{\rho} = \rho/\rho_\circ$) and find a non-singular solution which can be approximated for $\tilde{r} < 2$ by (for details see Binney & Tremaine 1987)

$$\tilde{\rho}(\tilde{r}) = \frac{1}{(1 + \tilde{r}^2)^{3/2}} \quad \text{for } \tilde{r} < 2 \qquad (15)$$

and for $\tilde{r} \gg 2$ with the singular function given in Eq. (14).

An observable quantity, connected with the surface density of stars in a cluster, is the surface brightness. The luminosity function $\Phi(M)$ gives the relative number of stars with absolute magnitude M in the range $[M - 1/2, M + 1/2]$. The number surface density of the stars can be computed from the observed surface brightness. Assuming that all stars in the cluster have the same mass, we can compare the above densities with surface brightness measurements. The mass surface density Σ is derived from the mass density by the integration

$$\Sigma(b) = \int_{-\infty}^{\infty} \rho(\sqrt{l^2 + b^2})dl\,, \qquad (16)$$

where b is the projected radial distance. For the density of the singular isothermal sphere, given by Eq. (14), the surface density is

$$\Sigma(b) = \frac{\sigma^2}{2Gb}\,. \qquad (17)$$

Similarly, the density $\tilde{\rho}(\tilde{r})$ in Eq. (15) leads to the surface density

$$\Sigma(b) \propto \frac{2}{1+\tilde{b}^2} \, , \tag{18}$$

where $\tilde{b} = b/r_c$.

Since Eq. (15) fits the regular solution of Eq. (13) in the range $\tilde{r} < 2$, we find that the corresponding surface density falls to roughly half of its central value at the core radius r_c. Knowing r_c and σ from observations, the central density $\rho_\circ$ is determined in the isothermal model by

$$r_c = \sqrt{\frac{9\sigma^2}{4\pi G \rho_\circ}} \, . \tag{19}$$

With $r_c = 0.52\,\text{pc}$ as given in Lang (1992) and a velocity dispersion of $\sigma = 10\,\text{km/s}$ (Binney & Tremaine 1987), Eq. (19) for 47 Tuc yields $\rho_\circ = 6.0 \times 10^4\,\text{M}_\odot/\text{pc}^3$.

King (1962) found that the above surface density functions (17), (18) fit well star counts up to a limiting radius r_t (called tidal radius), where the measured surface density drops sharply to zero. Thus a better fit to the surface density of the cluster is given by

$$\Sigma(b) \propto \left(\frac{1}{[1+(b/r_c)^2]^{1/2}} - \frac{1}{[1+(r_t/r_c)^2]^{1/2}} \right)^2 . \tag{20}$$

With a spherical symmetric density

$$\rho(r) = -\frac{1}{\pi} \int_r^{r_t} \left[\frac{d}{db}\Sigma(b) \right] \frac{db}{(b^2 - r^2)^{1/2}} \, , \tag{21}$$

the corresponding mass density becomes

$$\rho(r) = \frac{k}{\pi r_c [1+(r_t/r_c)^2]^{3/2}} \frac{1}{z^2} \left[\frac{1}{z}\arccos z - (1 - z^2)^{1/2} \right] , \tag{22}$$

where

$$z = \left[\frac{1 + (r/r_c)^2}{1 + (r_t/r_c)^2} \right]^{1/2}$$

and k is chosen such that $\rho(0) = \rho_\circ$ (King 1962). Integrating this density with a tidal radius $r_t = 60.3\,\text{pc}$ (Lang 1992), one finds a total mass of $M_{\text{tot}}^{\text{King}} = 3.5 \times 10^5\,M_\odot$ for 47 Tuc.

To study the dependence of the optical depth and the lensing rate on different mass distributions, we will use the following four models (see Fig. 1).

1. **Fitted King model:** the density is given by Eq. (22) with central density $\rho_\circ = 6.0 \times 10^4\,\frac{\text{M}_\odot}{\text{pc}^3}$, core radius $r_c = 0.52$ pc and $M_{\text{tot}}^{\text{King}} = 3.5 \times 10^5\,\text{M}_\odot$ as already mentioned above.
2. **Inner isothermal model:** the density is given by Eq. (15) with $r_c = 0.52$ pc and $\sigma = 10$ km/s as above, but with $\rho_\circ$ chosen such that the total mass within the tidal radius is the same as in the fitted King model, rather than determined via Eq. (19).

3. **Singular model:** the mass density is described by the isothermal sphere, i.e. by Eq. (14) with the same σ as mentioned above. The total mass of this model within the tidal radius r_t is $M_{\text{tot}}^{\text{sing}} = 2.8 \times 10^6\,\text{M}_\odot$.
4. **$\frac{1}{1+\mathbf{r}^2}$ - model:** the mass density is given by

$$\rho(r) = \frac{\rho_\circ}{1 + \left(\frac{r}{r_c}\right)^2} \tag{23}$$

with r_c as above and $\rho_\circ$ chosen such that the total mass within the tidal radius is the same as for the fitted King model.

The last three mass distributions are cutted discontinuously at the tidal radius. Thus the integration range for the optical depth and the lensing rate is only a sphere with a radius equal to the tidal radius. For all models the velocity distribution follows a Maxwell distribution as in Eq. (11) with $\sigma = 10\,\text{km/s}$.
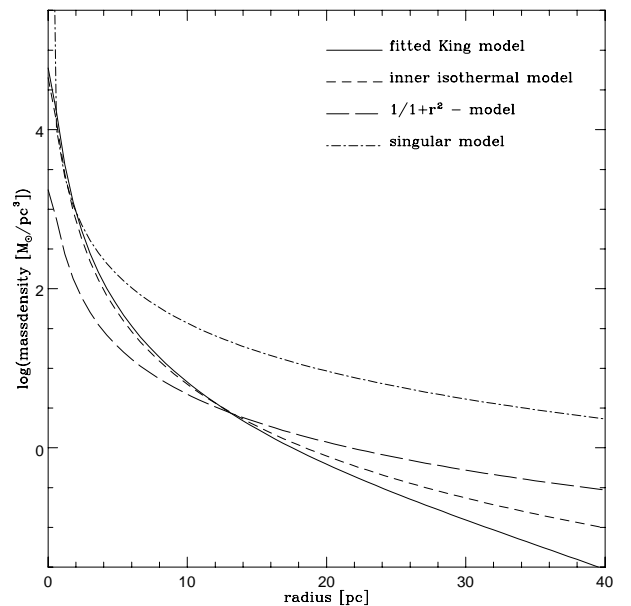

Fig. 1. The four different mass density models used in the calculations, plotted as a function of the radial distance r. For clarity the plot ends at $r = 40\,\text{pc}$ rather than at $r = r_t = 60.3\,\text{pc}$.

The $\frac{1}{1+r^2}$-model is considered mainly because the integrations can be performed analytically. Hence, we can easily compare the analytic result with the ones obtained numerically for the other models.

Of course there exist more sophisticated models for globular clusters, e.g. the (single or multimass) King-Michie models (King 1966, Gunn & Griffin 1979), that take into account the finite escape velocity from the cluster, which naturally leads to a finite extension of the cluster. However, for the study of the influence of different

mass distributions on the measured quantities, we consider the above mentioned models to be sufficient and, therefore, in this section, restrict our discussion to them. In addition, we remind on the well known scaling properties of the King model, which allow to derive the corresponding quantities for a different choice of parameters.

3.2. Optical depth, lensing rate and mean event duration for SMC-47 Tuc

We now discuss the different possibilities for microlensing in the system SMC-47 Tuc, i.e. events where the source and the lens are both located in 47 Tuc; the source is in the SMC and the lens in 47 Tuc; the source is in 47 Tuc and the lens in the halo of the Milky Way, or finally the source resides in the SMC and the lens in the Milky Way. For SMC self-lensing we refer e.g. to the paper by Palanque-Delabrouille, Afonso, Albert et al. (1997).

At the end we also discuss the dependence on the mass function, which itself is independent of the lensing geometry. Since we hope to disentangle the different cases, we also calculate the differential rate $\frac{d\Gamma}{dT}$. Throughout this part we will assume all lenses to have the same mass. The velocity distribution of the halo objects, as well as those of the cluster is taken to be a Maxwell function. As already mentioned, we define the amplification threshold to be $A_{TH} = 1.34$.

3.2.1. Optical depth for source and deflecting mass in the cluster

For completeness we discuss also this case, although, as we will see, its contribution can be neglected for all practical purposes.

For a pointlike source τ_{opt} is, according to Eq. (3), given by

$$\tau_{opt} = \int_{x_b}^{1} \frac{4\pi G}{c^2} D^2 x(1-x)\rho_d(r(x)) \; dx \qquad (24)$$

where

$$x_b = \frac{D_c - \sqrt{r_t^2 - b^2}}{D} \simeq 1 - \frac{r_t}{D} = 1 - 1.4 \times 10^{-2} \,. \qquad (25)$$

D_c is the distance from the observer to the cluster center and D the one to the source. Hence, the integration is cut at the boundary of the cluster. The optical depth for a source located in the center of the cluster ($b = 0$) is $\tau_{opt} = 9.2 \times 10^{-9} \frac{M_{dark}}{3.5 \times 10^5 \, M_\odot}$ for the fitted King model. The results for the 4 different models are shown in Fig. 2. Of course the isothermal-sphere model differs most, because its total mass $M_{tot}^{sing} = 2.8 \times 10^6 M_\odot$ varies substantially from the others.

Since the lower limit of integration is very close to 1, τ_{opt} can be approximated as follows

$$\tau_{opt} \simeq \frac{4\pi G}{c^2} \int_{0}^{x_u} l \; \rho_d(r(l)) \; dl \,.$$
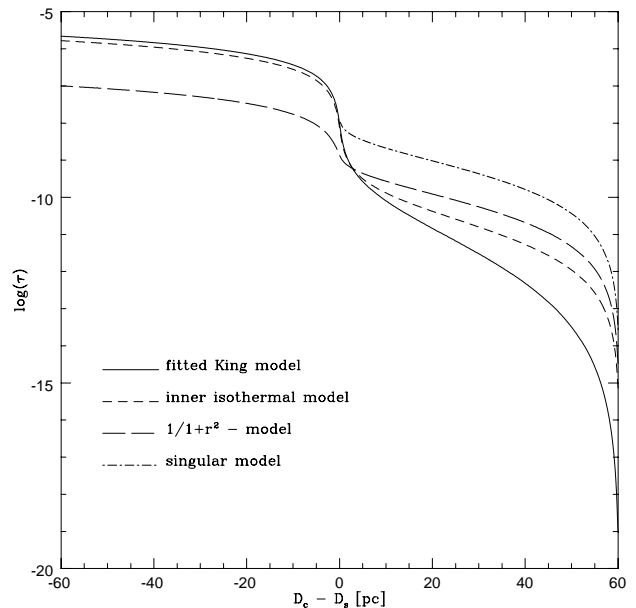

Fig. 2. The optical depth for the four different models as a function of the source position. All sources are located on the line of sight from the observer to the cluster center, but at different radii relative to the center. The optical depth of the singular model is only shown for sources with $D_c - D > 0$, since its mass density has a singularity at $r = 0$. For the plot we assume $f = 1$, and the total mass of the models as given in Sect. 3.

Here

$$x_u = \sqrt{r_t^2 - b^2} - (D_c - D)$$

and $l = D - D_d$ is the distance from the lens (located at D_d) to the source. Hence, τ_{opt} is proportional to $D - D_d$ weighted with the mass density in the globular cluster along the line of sight from the observer to the source.

3.2.2. Lensing rate for source and deflecting mass in the cluster

We assume the mass function to be independent of the position and all lenses are taken to have the same mass $\mu_\circ$ (in units of $M_\odot$). From Eq. (9) we find that the transverse velocity distribution is given by

$$f_T(v_T) = 2\frac{v_T}{v_H^2}e^{-v_T^2/v_H^2} \qquad (26)$$

with $v_H^2 = 2\sigma^2$. If the source as well as the deflecting mass are in the cluster, the event rate becomes

$$\Gamma = \frac{\sqrt{2\pi}\sigma r_E}{M_\odot\sqrt{\mu_\circ}} D \int_{x_b}^{1} \rho_d(r(x)) \sqrt{x(1-x)}dx \,, \qquad (27)$$

with $r(x) = \sqrt{b^2 + (D_c - xD)^2}$ and r_E defined to be

$$r_E = \sqrt{\frac{4G}{c^2} M_\odot D}\,. \tag{28}$$

We use the same geometry as in the previous subsection. The result for the fitted King model for a source located at the center of the cluster is $\Gamma = \frac{6.6 \times 10^{-15}}{\sqrt{\mu_\circ}} \frac{M_{\text{dark}}}{3.5 \times 10^5 M_\odot}$ 1/s.

In order to more easily compare between the microlensing rates for different locations of the source and the lens, we introduce the quantity $\tilde{n}(\alpha)$:

$$\tilde{n}(\alpha) \equiv \frac{\tilde{N}(\alpha)}{(1')^2}\,,$$

where $\tilde{N}(\alpha)$ is the number of microlensing events per unit time in an area of $(1')^2$ located at an angular distance α from the cluster center. For simplicity, we will give the rate $\tilde{n}(\alpha)$ in units of pc. In the plane perpendicular to the line of sight through the cluster center, $1'$ corresponds to 1.2 pc. Hence, we can define a new quantity

$$n\left(b = \alpha \frac{1.2\,\text{pc}}{1'}\right) \equiv \tilde{n}(\alpha) \frac{1}{(1.2\,\text{pc})^2}\,,$$

which is in units of pc^{-2} unit time^{-1}. We call $n(b)$ the surface density of microlensing events. To calculate $n(b)$ we have to add up the lensing rates for all stars located on the line of sight with impact parameter b from the cluster center. From Eq. (27), we see that the lensing rate Γ depends on D and on b, through $r(x)$ and x_b. Taking this into account we get

$$n(b) = \int_{D^i}^{D^f} n_{\text{star}}(\sqrt{b^2 + (D_c - D)^2})\, \Gamma(D,b)\, dD \tag{29}$$

where in the ideal situation, which will lead to an upper bound for $n(b)$ we have $D^{f,i} = D_c \pm \sqrt{r_t^2 - b^2}$. $n_{\text{star}}(r)$ is the number density of stars (in units of pc^{-3}) in the cluster at distance r from the center and D, b, D_c are all in units of pc. To describe the distribution of stars in the cluster, we assume that the number density is proportional to the mass density ρ_{King} of the fitted King model, since the mass surface density of this model is proportional to the number surface density of stars in a cluster. Thus n_{star} is given by

$$n_{\text{star}}(r) = \frac{N_{\text{star}}}{M_{tot}^{\text{King}}}\, \rho_{\text{King}}(r) \tag{30}$$

with $N_{\text{star}} = 4.6 \times 10^5$ (Lang 1992). With Eqs.(27) and (29) this leads to

$$n(b) = 3.6 \times 10^{-19} \frac{N_{\text{star}}}{M_{\text{tot}}} \frac{1}{\sqrt{\mu_\circ}}$$
$$\times \int_{D^i}^{D^f} D^{3/2} \rho_{\text{King}}\left(\sqrt{b^2 + (D_c - D)^2}\right)$$
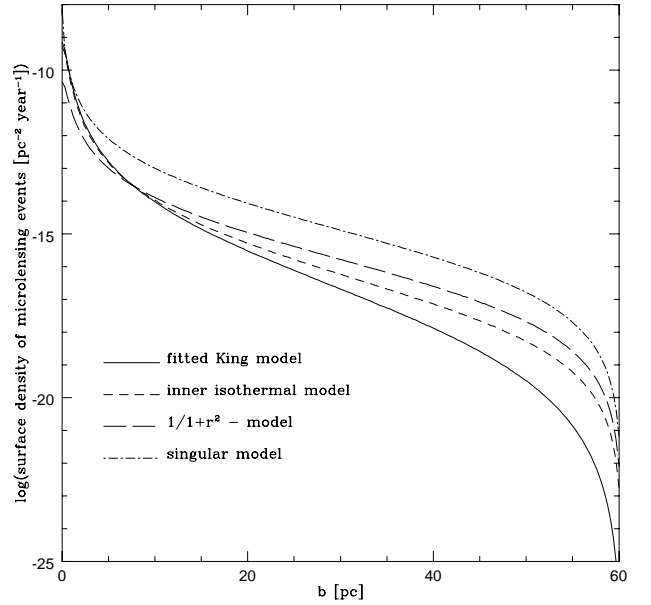$$\times \int_{x_b(D)}^{1} \sqrt{x(1-x)} \rho_d\left(\sqrt{b^2 + (D_c - xD)^2}\right)\, dD\, dx\,.$$

Fig. 3. The surface density of microlensing events is plotted as a function of the projected radius b for the four different models calculated in the text, assuming $\mu_\circ = 1$. For the plot we assume $f = 1$, and the total mass of the models as given in Sect. 3.

The results for the four models are shown in Fig. 3.

The number of lensing events per year in the whole cluster is

$$\int_0^{r_t} 2\pi\, n(b) b\, db = 2 \times 10^{-2} \sqrt{\frac{1}{\mu_\circ}}\, f\, \frac{N_{\text{star}}}{4.6 \times 10^5} \tag{31}$$

for the fitted King model. On the other hand, the number of lensing events depends also on the telescope resolution. Assuming a distribution according to Eq. (30), we find that stars with a projected radial distance smaller than 0.6 pc from the center cannot be resolved if the limiting resolution of the telescope is 0.1", whereas if it is 1" even stars with projected radius b smaller than 7.5 pc from the center cannot be resolved. Hence, the number of expected lensing events per year using a telescope with a resolution of 0.1" is

$$\int_{0.6\text{pc}}^{r_t} 2\pi\, n(b) b\, db = \begin{cases} 1.1 \times 10^{-2} \sqrt{\frac{1}{\mu_\circ}} \frac{M_{\text{dark}}}{3.5 \times 10^5 M_\odot} \frac{N_{\text{star}}}{4.6 \times 10^5} \\[2ex] 2.4 \times 10^{-3} \sqrt{\frac{1}{\mu_\circ}} \frac{M_{\text{dark}}}{3.5 \times 10^5 M_\odot} \frac{N_{\text{star}}}{4.6 \times 10^5} \end{cases}$$

and the one for a resolution of 1" is

$$\int_{7.5\text{pc}}^{r_t} 2\pi\, n(b) b\, db = \begin{cases} 1.4 \times 10^{-4} \sqrt{\frac{1}{\mu_\circ}} \frac{M_{\text{dark}}}{3.5 \times 10^5 M_\odot} \frac{N_{\text{star}}}{4.6 \times 10^5} \\[2ex] 2.3 \times 10^{-4} \sqrt{\frac{1}{\mu_\circ}} \frac{M_{\text{dark}}}{3.5 \times 10^5 M_\odot} \frac{N_{\text{star}}}{4.6 \times 10^5} \end{cases}$$

The first line is for the fitted King model, the second for the $\frac{1}{1+r^2}$-model.

The distribution of the microlensing events as a function of their duration T, using the transverse velocity distribution as defined in Eq. (26) and the definition of r_E in Eq. (28), is given by

$$\frac{d\Gamma}{dT} = -\frac{2D\mu_\circ}{M_\odot} \frac{r_E^4}{\sigma^2} \frac{1}{T^4}$$
$$\times \int (x(1-x))^2 \, \rho_d(x) \exp\left[-\frac{R_E^2(x)}{2\sigma^2 \, T^2}\right] \, dx. \qquad (32)$$

The result for the fitted King model assuming a lens mass $\mu_\circ = 1$ is shown in Fig. 4.
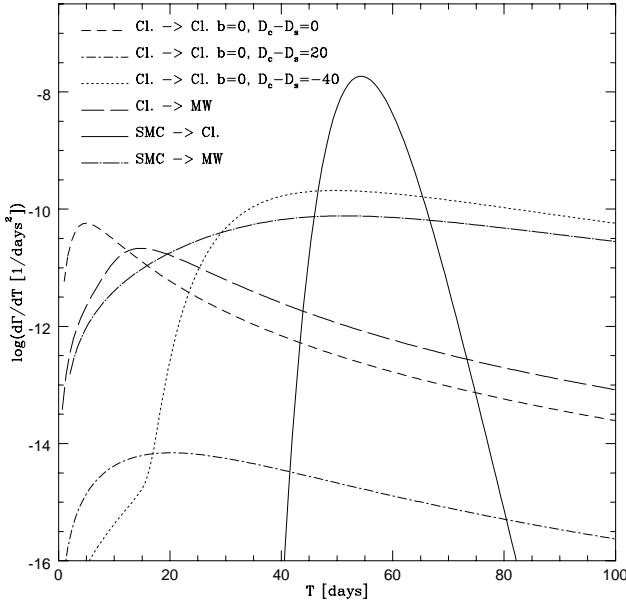

Fig. 4. The distribution of the lensing events with duration $T = R_E/v_T$ for different geometries of the lens system. For the calculations we used the fitted King model and made the assumption that all lenses have the same mass $\mu_\circ = 1$. The notation is to be understood as follows: the first entry denotes the position of the source, the second the one of the lens e.g. SMC−>Cl means a star of the SMC is lensed by an object in the cluster. MW abbreviates Milky Way; b, D_c and D are defined within the text. For the plot we assume $f = 1$, and the total mass of the model as given in Sect. 3.

3.2.3. Optical depth and lensing rate for the source in the SMC and the deflecting mass in the cluster

What changes in the calculation of τ_{opt} and Γ is itemized below:

- the distance D of the source is now about $63\,\mathrm{kpc}$, corresponding to the distance of the SMC from the Sun;
- the x-integration goes from $x_i = (D_c - \sqrt{r_t^2 - b^2})/D$, to $x_f = (D_c + \sqrt{r_t^2 - b^2})/D$;
- the velocity distribution gets shifted, because of the motion of 47 Tuc relative to the SMC with a velocity of about $v_d \cong 180\,\mathrm{km/s}$. Hence, a velocity drift has to be introduced in the Maxwell distribution, such that

$$f(\boldsymbol{v}) = \frac{1}{(2\pi\sigma^2)} \exp\left(-\frac{(v_x - v_d)^2 + v_y^2 + v_z^2}{2\sigma^2}\right) , \quad (33)$$

where we assume the x-axis to be parallel to the velocity drift. The resulting transverse velocity distribution is then given similarly to Eq. (26). With this, the integral over dv_T in Eq. (4) yields

$$\int_0^\infty v_T f(v_T) dv_T = v_d \simeq 180\,\mathrm{km/s} . \qquad (34)$$

Thus, the lensing rate and the optical depth become

$$\tau_{opt} = \frac{4\pi G}{c^2} D^2 \int_{x_i}^{x_f} x(1-x)\rho_d(r(x))dx , \qquad (35)$$

$$\Gamma = \frac{2v_d r_E}{M_\odot \sqrt{\mu_\circ}} D \int_{x_i}^{x_f} \sqrt{x(1-x)} \, \rho_d(r(x))dx$$
$$= \frac{5.1 \times 10^{-18}}{M_\odot \sqrt{\mu_\circ}} \left(\frac{D}{\mathrm{pc}}\right)^{3/2} \int_{x_i}^{x_f} \sqrt{x(1-x)} \frac{\rho_d(r(x))}{M_\odot/\mathrm{pc}^3} dx . (36)$$

For the extreme case of a star in the SMC lying on the line of sight going through the center of the cluster, the optical depth is $\tau_{opt} = 1.4 \times 10^{-4} \frac{M_{dark}}{3.5 \times 10^5 M_\odot}$ and the lensing rate $\Gamma = 2.0 \times 10^{-11} \sqrt{\frac{1}{\mu_\circ}} \frac{M_{dark}}{3.5 \times 10^5 M_\odot} \, 1/\mathrm{s}$.

Since the tidal radius is smaller than about $200\,\mathrm{pc}$, the quantity $x(1-x)$ as well as $\sqrt{x(1-x)}$ does not vary more than 10% over the integration range, and the variation of τ_{opt} as well as Γ is directly proportional to the surface density of the cluster. Assuming a tidal radius of $60\,\mathrm{pc}$ we find (with $\bar{x}$ an average value for x)

$$\tau_{opt} = \bar{x}(1 - \bar{x}) \frac{4\pi G}{c^2} D \, \Sigma(b) \, f$$
$$= (2.32 \pm 0.04) \times 10^{-9} \left(\frac{D}{63\,\mathrm{kpc}}\right) \times \frac{\Sigma(b)}{(M_\odot/\mathrm{pc}^2)} \, f \quad (37)$$

$$\Gamma(b) = \sqrt{\bar{x}(1-\bar{x})} \, \frac{2v_d r_E}{M_\odot \sqrt{\mu_\circ}} \, \Sigma(b) \, f$$
$$= (3.25 \pm 0.03) \times 10^{-16} \sqrt{\frac{D}{63\,\mathrm{kpc}} \frac{\Sigma(b)}{M_\odot/\mathrm{pc}^2}} \, \sqrt{\frac{1}{\mu_\circ}} \, f . \quad (38)$$

The mean event duration is

$$\langle T \rangle = \frac{2}{\pi} \frac{\tau_{opt}}{\Gamma} = 52 \sqrt{\mu_\circ} \text{ days,}$$

which is nearly independent of the angle between source and cluster center, since both τ_{opt} and Γ are proportional to $\Sigma(b)$ as given by Eqs.(37) and (38).

Of course the chance to find a lensing event in this case depends not only on the optical depth, but also on the number of SMC stars in the background of 47 Tuc. Hesser, Harris, Vandenberg et al. (1987) finds an average of 1000 stars/30(arcmin)^2 with a magnitude in the interval of $0.0 < (B-V) < 0.8$, $21 < V < 24$. In the following we assume a constant number of 50 stars/(arcmin)^2, although there is a gradient in the density of the SMC stars across the whole 47 Tuc region decreasing from the southeast to the northwest side.

According to Eq. (29) we get with the above mentioned proportionality between Γ and Σ a surface density of microlensing events of

$$n(b) = \sqrt{\bar{x}(1-\bar{x})} \, \frac{2v_d r_E}{M_\odot \sqrt{\mu_\circ}} \, \Sigma(b) \, \frac{n_{\text{star}}}{(1.2\,\text{pc})^2} \, f \,, \qquad (39)$$

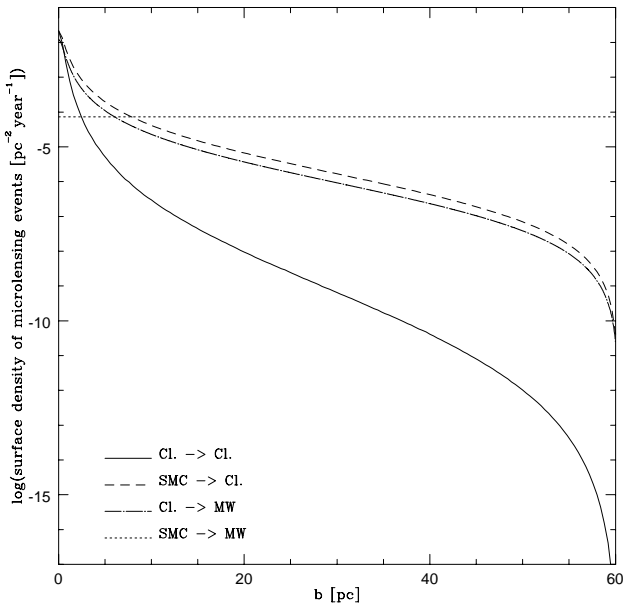where n_{star} is the number of SMC stars per $(1')^2$. $n(b)$ is shown in Fig. 5.

Fig. 5. The surface density of microlensing events is shown for the different geometries of the lens system. For the calculations we used the fitted King model and made the assumption, that all lenses have the same mass $\mu_\circ = 1$. For the abbreviations we refer to Fig. 4. For the plot we assume $f = 1$, and the total mass of the models as given in Sect. 3.

The number of events per year in the whole area of 47 Tuc is then given by

$$\int_0^{r_t} 2\pi \, n(b) \, b \, db =$$
$$= 0.12 \, \sqrt{\frac{1}{\mu_\circ}} \, \frac{M_{\text{dark}}}{3.5\times10^5 M_\odot} \, \frac{n_{star}}{50/(1.2\text{pc})^2} \, \frac{1}{\text{year}} \qquad (40)$$

for the fitted King model. The expected number of events per year for an observation done with a resolution of $0.1''$ is

$$\int_{0.6\text{pc}}^{r_t} 2\pi \, n(b) \, b \, db = \begin{cases} 1.0 \times 10^{-1} \, \sqrt{\frac{1}{\mu_\circ}} \, \frac{M_{\text{dark}}}{3.5\times10^5 M_\odot} \, \frac{n_{\text{star}}}{50} \\[2ex] 1.2 \times 10^{-1} \, \sqrt{\frac{1}{\mu_\circ}} \, \frac{M_{\text{dark}}}{3.5\times10^5 M_\odot} \, \frac{n_{\text{star}}}{50} \end{cases}$$

and for an observation with a resolution of $1''$

$$\int_{7.5\text{pc}}^{r_t} 2\pi \, n(b) \, b \, db = \begin{cases} 3.0 \times 10^{-2} \, \sqrt{\frac{1}{\mu_\circ}} \, \frac{M_{\text{dark}}}{3.5\times10^5 M_\odot} \, \frac{n_{\text{star}}}{50} \\[2ex] 1.0 \times 10^{-1} \, \sqrt{\frac{1}{\mu_\circ}} \, \frac{M_{\text{dark}}}{3.5\times10^5 M_\odot} \, \frac{n_{\text{star}}}{50} \,. \end{cases}$$

The first value is for the fitted King-model and the second for the $\frac{1}{1+r^2}$-model.

For comparison, if we insert a velocity $v_d \simeq 180\,\text{km/s} = 9.2 \times 10^{-3}$ arcsec/year for the cluster and a density of 50 SMC stars per $(1')^2$ in the formula for the event rate per year, as given in the paper of Paczyński (1994) one obtains $f \times 1.5 \sqrt{\frac{1}{\mu_\circ}} \frac{1}{\text{year}}$ for the rate in the whole area of the cluster, $f \times 1.4 \sqrt{\frac{1}{\mu_\circ}} \frac{1}{\text{year}}$ for the rate with a resolution of 0.1" and $f \times 1.3 \sqrt{\frac{1}{\mu_\circ}} \frac{1}{\text{year}}$ for the rate with a resolution of 1". The factor f parametrizes the fraction of dark matter $f = M_{\text{dark}}/M_{\text{tot}}$. Paczyński used in his calculations the total mass as given by the singular isothermal sphere model, which gives $M_{\text{tot}} = 4.3 \times 10^6 M_\odot$. The difference to our values is mainly due to the different adopted mass surface densities. Since the total mass of the fitted King model is $M_{\text{tot}}^{\text{King}} = 3.5 \times 10^5 M_\odot$, this explains, with the help of Eq. (40), just the factor 12 between Paczyński's results for the number of events and ours for the fitted King model for the rate in the whole area of the cluster. A multi-mass model fitted to radial velocity and surface brightness observations of 47 Tuc leads to a total mass of $M_{tot} = 1.1 \times 10^6 M_\odot$ (Meylan 1989), which is about 3 times bigger than the value for the fitted King model. In addition, the fitted King model concentrates much more mass in the center, whereas in the singular isothermal sphere model, there is still a lot of mass in the outer regions of the cluster. From these considerations, we see that the uncertainties are quite important and they are mainly due to the poor knowledge of the dark matter content in globular clusters.

Paczyński (1994) proposed to measure the microlensing of background stars by MACHOs in globular clusters, because in this way the mass of the lens can be determined more precisely than in the lensing experiments under way. Since the lens is in the cluster, it has the transverse velocity and the position of the cluster. To estimate the inherent error of the method we adopt the values below, where the transverse velocity v_T is assumed to be precisely known up to the cluster dispersion velocity and the distance up to the cluster size: $v_T = 180\,\text{km/s} \pm 10\,\text{km/s}$,

$D_d = 4100 \, \text{pc} \pm 60 \, \text{pc}$ and $D = 63 \, \text{kpc} \pm 6 \, \text{kpc}$. It follows then an uncertainty in the mass determination of $\left| \frac{\Delta m}{m} \right| \leq 0.33$. The uncertainty in the lens mass with the currently reported lensing events is more like a factor 3 or even bigger (Jetzer & Massó 1994, Jetzer 1994).

The distribution of the lensing events as a function of the duration T is:

$$
\frac{d\Gamma}{dT} = -\frac{2D\mu_\circ}{\pi M_\odot} \frac{r_E^4}{T^4} \frac{1}{\sigma^2} \int_{x_E}^{x_b} dx \int_0^\pi dy \, [x(1-x)]^2 \, \rho_d(x)
$$
$$
\times \exp\left(-\frac{v_d^2}{2\sigma^2} - \frac{R_E^2}{2\sigma^2 T^2} + \frac{R_E \, v_d}{\sigma^2 T} \cos y \right) , \quad (41)
$$

where y is the angle between $\mathbf{v}_d$ and the projected MACHO velocity in the plane perpendicular to the line of sight. The numerical results, with the above mentioned values for v_d and σ are shown in Fig. 4.

3.2.4. Optical depth and lensing rate for the source in the cluster and the deflecting mass in the halo of the Milky Way

To calculate the optical depth and the lensing rate we set the position of the source equal to the position of the cluster. In the reference frame, where the origin is at the galactic center and the $x_1 - x_2$ plane is the symmetry plane of the galaxy, the coordinates of a lens, located on the line of sight from the observer to the cluster center, are $x_1 = xD_c \cos b_T \cos l_T - R_{GC}$, $x_2 = xD_c \cos b_T \sin l_T$, and $x_3 = xD_c \sin b_T$, where $b_T = 44.89^o$ and $l_T = 305.9^o$ are the galactic latitude and longitude of 47 Tuc. With the number density distribution Eq. (5), we find the optical depth (with $D = D_c$) to be $\tau_{opt} = 1.5 \times 10^{-8}$.

Let's now look at the lensing rate. Since the velocity distribution in the halo is assumed to be Maxwellian, the integration over v_T in Eq. (9) leads to

$$
\int v_T f(v_T) dv_T = \frac{v_H}{2} \sqrt{\pi} \qquad (42)
$$

with $v_H \simeq 210 \, \text{km/s}$. Thus, in a model where all lenses have the same mass, the lensing rate becomes with Eq. (4).

$$
\Gamma = 4.7 \times 10^{-15} \sqrt{\frac{1}{\mu_\circ}} \, 1/s \, . \qquad (43)
$$

According to Eq. (29) the surface density of microlensing events in this case is

$$
n(b) = \Gamma \, \frac{N_{\text{star}}}{M_{\text{tot}}} \, \Sigma_{\text{King}}(b) \, . \qquad (44)
$$

$\frac{N_{\text{star}}}{M_{\text{tot}}} \Sigma_{\text{King}}(b)$ is the number surface density of the stars in the cluster in units of pc^{-2}.

The time scale calculated with Γ and τ_{opt} as obtained above is

$$
<T> = \frac{2}{\pi} \frac{\tau_{opt}}{\Gamma} = 23 \, \sqrt{\mu_\circ} \, \text{days} \, .
$$

For the distribution of the lensing events we obtain

$$
\frac{d\Gamma}{dT} = -\frac{4D\mu_\circ}{M_\odot} \frac{r_E^4}{v_H^2} \frac{1}{T^4}
$$
$$
\times \int_0^1 dx \rho_d(x) [x(1-x)]^2 \exp\left(-\frac{R_E^2}{v_H^2 T^2} \right) \qquad (45)
$$

with the MACHO mass density $\rho(x)$ as in Eqs. (5) and (6).

$$
\frac{d\Gamma}{dT} = 3.0 \times 10^{-2} \frac{1}{T^4} \times
$$
$$
\int_0^1 dx \rho(x) [x(1-x)]^2 \exp\left(-2.3 \times 10^3 \frac{x(1-x)}{T^2} \right) \frac{1}{\text{days}^2} . \qquad (46)
$$

The numerical results with $v_H = 210$ km/s and $D = 4.1$ kpc for $\mu_\circ = 1$ are shown in Fig. 4 where the motion of the cluster relative to the Milky Way halo is neglected.

For a list of globular clusters which might be used as targets for a systematic microlensing search, we refer to the papers of Gyuk & Holder (1997) and Rhoads & Malhotra (1997).

3.3. Optical depth and lensing rate for a source in the SMC and the deflecting mass in the halo of the Milky Way

Since this is a standard case we restrict to the presentation of the results. With a distance $D = 63$ kpc and the galactic coordinates of the SMC $l = 302.8^\circ$ $b = -44.3^\circ$, we get for the optical depth and the lensing rate

$$
\tau = 7.0 \times 10^{-7} \text{ and } \Gamma = 6.6 \times 10^{-14} \sqrt{\frac{1}{\mu_\circ}} \, 1/s \, .
$$

Therefore, the time scale is $<T> = 78 \, \sqrt{\mu_\circ}$ days. The result for $\frac{d\Gamma}{dT}$ is shown in Fig. 4.

3.3.1. Dependence of the lensing rate Γ on the mass function

Up to now, we assumed all lenses in the cluster to have the same mass, which is, of course, rather unphysical. Therefore, we discuss now the variation of Γ with the mass function $dn/d\mu$. However, we will still make the assumption that the mass function does not depend on the position. To estimate the variation of Γ we choose a mass function of the form

$$
\frac{dn_\circ}{d\mu} = C\mu^{-(1+\gamma)} \qquad (47)
$$

with γ in the interval $[-1, 3]$ and the mass m in the range $m_a \leq m \leq m_b$. With Eq. (47) the lensing rate Γ becomes (with $u_{TH} = 1$)

$$
\Gamma = \Gamma_\circ \frac{M_\odot}{\rho_\circ^d} \int \mu^{1/2} \frac{dn_\circ}{d\mu} d\mu
$$
$$
= \Gamma_\circ \frac{1-\gamma}{m_b^{1-\gamma} - m_a^{1-\gamma}} \times \frac{m_b^{1/2-\gamma} - m_a^{1/2-\gamma}}{1/2 - \gamma} \qquad . \qquad (48)
$$

$\Gamma_\odot$ is the lensing rate computed under the assumption that all lenses have mass $\mu_\circ = 1$.

For the limiting cases $\gamma << 1/2$ and $\gamma >> 1$ this leads to a lensing rate

$$\Gamma = \Gamma_\odot \begin{cases} \frac{1}{\sqrt{m_a}} & \gamma >> 1 \\ \frac{1}{\sqrt{m_b}} & \gamma << 1/2 \,. \end{cases} \qquad (49)$$

In Fig. 6 $\Gamma/\Gamma_\odot$ is shown for different upper and lower limits of the MACHO mass.
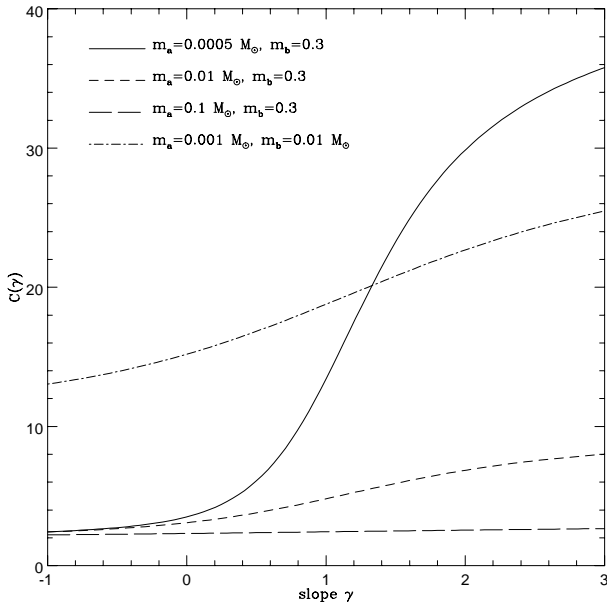

Fig. 6. $\Gamma/\Gamma_\odot$ is plotted as a funtion of the slope γ. This corresponds to the dependence of the lensing rate on the slope of the mass function. $\Gamma_\odot$ is the lensing rate for a model where all MACHOs have the same mass $\mu_\circ = 1$

4. Microlensing towards the bulge using dark objects in globular clusters as lenses

One encounters several problems by using globular cluster stars as sources. In fact, globular clusters have at most some 10^5 stars that can be monitored. The angular size of a globular cluster is small and the stars are highly concentrated towards the center. Furthermore, most globular clusters are located towards the galactic center which restricts the number of objects being well suited for an exploration of the halo. Therefore, microlensing by globular clusters only leads to valuable results, if one is able to simultanously observe dozens of clusters with a very high resolution for several years. At present this seems to be a somewhat to demanding task, however this could be feasible in the near future.

In this section we discuss the possibility to use dark objects in globular clusters towards the bulge as lenses (see also Taillet, Longaretti & Salati 1995, 1996), in front of rich regions of the galactic center or the spiral arms. There is a large sample of possible clusters which could be used for this purpose (see Table 1). The core radius of the dark component of the cluster can be larger than the core radius obtained by surface luminosity measurements. Since the size of the cluster is much smaller than its distance, it can be assumed to be equal for all its members, moreover, the velocity dispersion inside the cluster is also small, hence globular clusters are well suited for determining the lens mass.

4.1. Estimate of optical depth and event rate

In the first part of this section, we give some (conservative) estimates for the optical depth and the event rate due to some globular clusters towards the bulge by scaling the results obtained for 47 Tuc under the assumption that the clusters contain only little dark matter. As was derived in Eq. (39), the optical depth due to a globular cluster is proportional to the surface density of microlensing events and the pure geometrical quantity $\bar{x}(1-\bar{x})$. Assuming $\Sigma(b)$ to be proportional to the total visual magnitude M_V, we can calculate the contribution to the optical depth due to the clusters (see Table 1). Since the galactic bar is not too extended, we fix the distance of the sources to be 8.5 kpc.

Compared with the measured average optical depth towards the galactic center $\tau_{opt} \simeq 2.4 \times 10^{-6}$ due to the disk and the bar itself (Alcock, Allsman, Alves et al. 1997a), we see from Table 1 that some of the globular clusters can give a very significant contribution to the total optical depth or even dominate it along their line of sight, as in the case of NGC 6553, which lies close to the ideal distance of $\bar{x} = 0.5$.

A rough estimate of the microlensing event rate per year due to globular clusters towards Baades Window is obtained by properly rescaling Eq. (40). We compute the event rate in units of $\sqrt{\frac{1}{\mu_\circ}} \frac{M_{\mathrm{dark}}}{3.5 \times 10^5 M_\odot} \frac{n_{star}}{50/(1.2\mathrm{pc})^2} \frac{1}{\mathrm{year}}$ as in Eq. (40), in order to be able to easily compare between the different clusters. To that purpose one has to use the scaling factor η given by:

$$\eta = 0.12 \frac{v'_d r'_E}{v_d r_E} \frac{n'_{\mathrm{star}}}{n_{\mathrm{star}}} \frac{(1.2\,\mathrm{pc})^2}{A} \frac{\int \Sigma'(b)\, db}{\int \Sigma(b)\, db} \,, \qquad (50)$$

where the unprimed quantities belong to 47 Tuc and the primed to the cluster under consideration. A is the surface which corresponds to $(1')^2$ at the distance of the cluster. For the calculation of the numbers, as given in Table 1, we assumed $v'_d = 30\,\mathrm{km/s}$ which is indeed a very conservative value and, therefore, we will get a lower limit for the eventrate.

Object	Position $[l, b]$	M_V	$\bar{x}$	$\tau_{opt} \left[\frac{M_{\mathrm{dark}}}{3.5 \times 10^5 M_\odot} \right]$	N $\left[\sqrt{\frac{1}{\mu_\circ}} \frac{M_{\mathrm{dark}}}{3.5 \times 10^5 M_\odot} \frac{n_{star}}{50/(1.2\mathrm{pc})^2} \frac{1}{\mathrm{year}} \right]$
Terzan 1	357.57 1.00	-3.3	0.765	2.1×10^{-7}	1.1×10^{-5}
Terzan 5	3.81 1.67	-7.9	0.941	4.7×10^{-6}	5.5×10^{-4}
Terzan 6	358.57 -2.16	-6.8	0.882	3.2×10^{-6}	2.2×10^{-4}
UKS 1	5.12 0.76	-6.2	0.882	1.8×10^{-6}	1.3×10^{-4}
Terzan 9	3.60 -1.99	-3.9	0.918	1.6×10^{-7}	1.4×10^{-5}
Terzan 10	4.42 -1.86	-7.8	0.988	9.0×10^{-7}	4.3×10^{-4}
NGC 6522	1.02 -3.93	-7.5	0.824	8.6×10^{-6}	5.0×10^{-4}
NGC 6528	1.14 -4.17	-6.7	0.871	3.2×10^{-6}	2.1×10^{-4}
NGC 6540	3.29 -3.31	-5.3	0.412	1.9×10^{-6}	2.6×10^{-4}
NGC 6544	5.84 -2.20	-6.5	0.294	4.9×10^{-6}	1.5×10^{-3}
NGC 6553	5.25 -3.02	-7.7	0.553	1.8×10^{-5}	1.3×10^{-3}
NGC 6558	0.20 -6.03	-6.1	0.753	3.0×10^{-6}	1.6×10^{-4}

Table 1. Optical depth and event rate due to MACHOs in some globular clusters for sources located towards the galactic center. The symbols are defined within the text. Cluster data is adopted from Harris (1996).

4.2. Spatial distribution of microlensing events around NGC 6522, NGC 6528 and NGC 6540

In the following we present a rough analysis of the microlensing events around the three globular clusters which lie within the observation fields of MACHO and OGLE.

Within a radius of 30 pc around NGC 6522 and 6528 we found 7 events for each of them (see Table 2). Since the projected areas of these two clusters overlap, 4 events lie within the 30 pc circles around both clusters. NGC 6540, which is nearer to us, hosts a total of 15 events within the 30 pc circle. At first sight, since the covered area is about four times larger, this value seems to be lower than expected. However, NGC 6540 is about 8 times less bright than NGC 6522. Therefore, if the total luminosity roughly scales with the total mass content, we expect NGC 6540 to contain less dark matter than NGC 6522.

Within 12 pc we found 3 events for NGC 6522, 2 events for NGC 6528 and 4 events for NGC 6540 (see Table 2). The event rate ratio in units of events per square degree for the 12 pc circle and the 30 pc ring (excluding the innermost 12 pc) are 99/25 for NGC 6522, 74/35 for NGC 6528 and 33/17 for NGC 6540, respectively. For all three clusters the central region shows an increase in microlensing events. Due to the fact that the 30 pc circles around NGC 6522 and NGC 6528 intersect, we can also calculate the event rate in the overlapping region, which we find to be 70 events per square degree. Within our poor statistics, this is what one expects for a line of sight crossing twice the region of influence of a globular cluster. It would also give a first hint, that globular clusters can indeed have a population of dark objects that reaches out as far as 30 pc.

Of course, there is now the problem how to distinguish between the events due to MACHOs located in the globular cluster and those due to MACHOs in the disk or bulge, which will define our "background". Since this cannot be decided for a single event, we assume that the events which lie in the ring from 12 to 30 pc are due to MACHOs in the disk or bulge. This way we certainly overestimate the "background". Moreover, the common events within 30 pc around both NGC 6522 and NGC 6528 were counted as "background" events for both clusters. This way leading also to a higher background rate. The so estimated event rate per area is then subtracted from the value in the inner 12 pc region. The leftover events should be due to MACHOs located in the globular cluster. We find the following values (in parenthesis the "background"): 2 (1) hence a total of 3 events for NGC 6522, 1 (1) event for NGC 6528 and 2 (2) events for NGC 6540. We see that the number of observed events in the inner 12 pc is roughly twice as high as one would get due to MACHOs in the disk or bulge alone. By assuming that all the events in the ring from 12 to 30 pc are due to MACHOs in the disk or bulge, we have certainly underestimated the contribution from the globular cluster, since some of these events might also be associated with the cluster.

Of course, we must discuss the shortcomings of our analysis. We tacitly assumed that the product of total observation time and background star density is the same for the 12 and 30 pc regions for a given cluster. This should at least be well fullfilled for the relatively small regions around NGC 6522 and NGC 6528. For NGC 6522 and NGC 6528 we added MACHO and OGLE data, hence we use a different normalisation for them than for NGC 6540. In addition, we did not take into account the different efficiencies. Moreover, our evaluation is based upon a very poor statistics, and thus one must take the above results with all the necessary caution. However, since all our estimates were performed very conservatively and for all three clusters we get the same behaviour and since also the overlapping region of NGC 6522 and NGC 6528
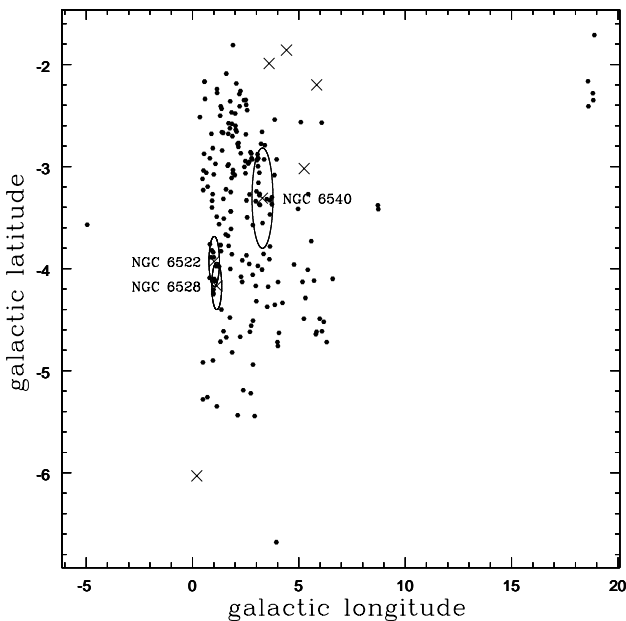
it is not possible to distinguish them, we have just taken the average value as a first approximation. This should not be far from the true value (as can be seen by inspection of Table 2). The results are given in Table 3. We see that depending on v_d the MACHOs can be either Jupiter type objects, brown dwarfs, M-stars or even white dwarfs.

Object	$\langle M \rangle$ $d \leq 12\,\mathrm{pc}$	$\langle M \rangle$ $12 < d \leq 30\,\mathrm{pc}$
NGC 6522	$0.003\,M_\odot$	$0.021\,M_\odot$
	$0.11\,M_\odot$	$0.75\,M_\odot$
NGC 6528	$0.021\,M_\odot$	$0.018\,M_\odot$
	$0.77\,M_\odot$	$0.65\,M_\odot$
NGC 6540	$0.003\,M_\odot$	$0.016\,M_\odot$
	$0.12\,M_\odot$	$0.57\,M_\odot$

Table 3. Typical masses for the microlensing events around NGC 6522, NGC 6528 and NGC 6540. The upper value corresponds to $v_d = 30\,\mathrm{km/s}$, the lower to $v_d = 180\,\mathrm{km/s}$. d denotes the distance from the cluster center.

Fig. 7. Position of 195 microlensing events towards the bulge in galactic coordinates (taken from the alert list of the MACHO collaboration and the corresponding list of the OGLE team). The crosses denote the position of some of the globular clusters reported in Table 1, which are located in Baades Window. Only the three clusters NGC 6522, NGC 6528 and NGC 6540 lie within the observation fields. The circles around the three clusters correspond to a radius of 30 pc around the cluster center.

shows an increase in microlensing events, we think it's fair to state, that globular clusters can –within some pc– at least double the optical depth and also the event rate due to MACHOs in the disk and the bulge; the latter quantities being $\tau \simeq 2.4 \times 10^{-6}$ (Alcock, Allsman, Alves et al. 1997a) and $\Gamma \simeq 1.3 \times 10^{-12} s^{-1}$ for a typical mass of $0.1\,M_\odot$.

Stars in globular clusters can also act as sources for microlensing, however, as discussed in Sect. 3.2.4 their contribution, unless for the very central region of $\sim 1 - 2\,\mathrm{pc}$, is very small as compared with lensing due to sources in the bulge. For NGC 6522 and NGC 6528 there is a small probability that the source lies in NGC 6528 and the lens in NGC 6522. Knowing the distances and the relative motion of the two clusters this system might yield the most accurate mass determination for a lensing object.

It is interesting to note, that the above mentioned event rate ratios scale with the total luminosity i.e. the brightest cluster NGC 6522 shows also the largest increase of events towards the center.

For the mean event duration as given in Table 2, we calculate the typical mass of a MACHO for $v_d = 30\,\mathrm{km/s}$ and $v_d = 180\,\mathrm{km/s}$. Obviously, one should consider only the events due to MACHOs in the cluster. However, since

Below we compute the optical depth and the event rate for four different King models as a function of the distance from the cluster center in the lens plane. The parameters are tuned such that the average of the values in the interval from 1 to 12 pc roughly corresponds to the above mentioned values for the optical depth τ and the event rate Γ. The tidal radius was assumed to be $r_t = 60.3\,\mathrm{pc}$, the distance to the lens is set to be 3.5 kpc and the one to the source 8.5 kpc. For the calculation of the event rate we again take the rather low value $v_d = 30\,\mathrm{km/s}$. Since we are not able to reproduce the mass function, we rather study a bi-mass model, hence the cluster consists of a heavy component (component 1) and a light one described by one of the other components as defined below.

Component 1: the density is given by Eq. (22) with central density $\rho_\circ = 6.0 \times 10^4\,\frac{M_\odot}{\mathrm{pc}^3}$ core radius $r_c = 0.52$ pc and $M_1^{\mathrm{King}} = 3.5 \times 10^5\,M_\odot$. For the calculation of the event rate we assumed a typical mass $M = M_\odot$.

Component 2: as Component 1, but with a core radius $r_c = 1.56$ pc and a typical mass of $M = 0.1\,M_\odot$. The total mass of this component is again $3.5 \times 10^5\,M_\odot$.

Component 3: as Component 2, but with a total mass of the component of $1.75 \times 10^6\,M_\odot$

Component 4: as Component 3, but with a core radius $r_c = 2.6$ pc

We find that a population of low mass objects as described by a King model with a total mass of $1.75 \times 10^6\,M_\odot$ can lead to the desired enhancement of the optical depth and the lensing event rate up to distances of $\sim 12\,\mathrm{pc}$ from the cluster center (see Figs. 9 and 10). Of course, the models and mass values given above have to be taken as an illustration, nevertheless it is clear that the rather high ob-

Object	Position [l, b]	M_V	within 12 pc	within 30 pc	Duration [days]	Mean [days]	Events/degree^2
NGC 6522	1.02 -3.93	-7.5	OGLE 5		12.4		
			97-37*		12		
			97-68		6		
						10.1	99
				OGLE 1*	25.9		
				OGLE 2	45		
				OGLE 4*	14		
				97-14*	21.5		
						26.6	25
NGC 6528	1.14 -4.17	-6.7	OGLE 1*		25.9		
			97-14*		21.5		
						23.7	74
				OGLE 3	10.7		
				OGLE 4*	14		
				OGLE 10	61.1		
				97-37*	12		
				95-11	30.5		
						22	35
NGC 6540	3.29 -3.31	-5.3	96-6, $d < 6$ pc		19.5		33
			96-17		16.5		
			95-29		12		
			95-40		8.5		
						14	33
				96-14, $d < 18$ pc	12.5		
				95-26, $d < 18$ pc	19.5		
				95-31, $d < 18$ pc	16		20
				97-2, $d < 24$ pc	23.5		
				97-10, $d < 24$ pc	8.5		
				97-24, $d < 24$ pc	5		
				95-36, $d < 24$ pc	12		20
				98-1	97.5		
				97-58	26.5		
				96-1	76		
				95-30	33.5		15
						30	17

Table 2. Microlensing events within a radial distance of 30 pc around NGC 6522, NGC 6528 and NGC 6540. Values marked with an asterisk lie within 30 pc of both NGC 6522 and NGC 6528. For NGC 6540 we also give the finer binning as used for Fig. 8. Data is taken from the alert list of the MACHO collaboration and the event list of the OGLE team. The event duration follows the OGLE convention i.e. $T = R_E/v_T$, which is half the value as reported in the MACHO alert list.

served microlensing rate of the clusters imply a substantial dark matter component. Although there is a large inherent uncertainty in the event rate due to the poor knowledge of v_d, it is important to note, that the required optical depth and event rate cannot be due to the heavy component alone.

5. Summary

We discussed in detail microlensing by globular clusters. 47 Tuc was taken as an example for which we performed the calculation of the optical depth, the microlensing event rate and the average lensing duration for all possible geometries of the system SMC-47 Tuc-Milky Way. In addition, we studied the dependence of these parameters on the mass function.

We have seen that for the case, where the source is a star in the SMC and the lens is a MACHO in 47 Tuc, one can expect an observable eventrate of $\sim 0.1 - 1$ per year. However, this result depends crucially on the total amount of dark matter and its distribution in the cluster, which both are not well known at present.
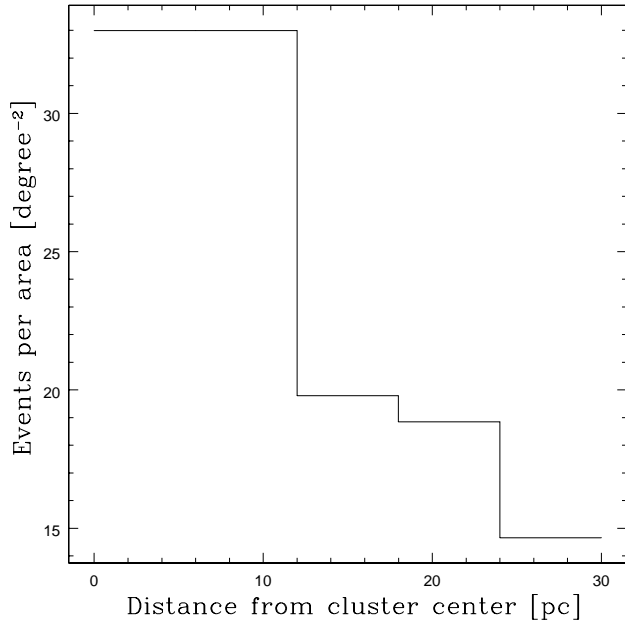
Fig. 8. The microlensing event rate per area as a function of the radial distance from the cluster center for NGC 6540.
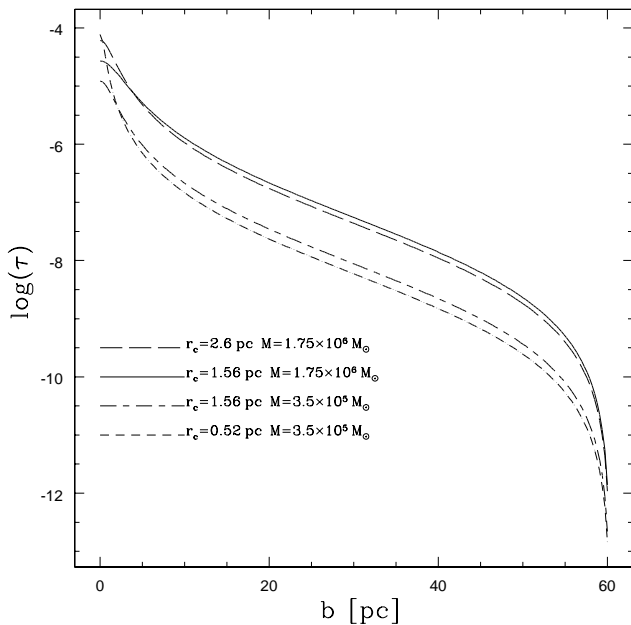

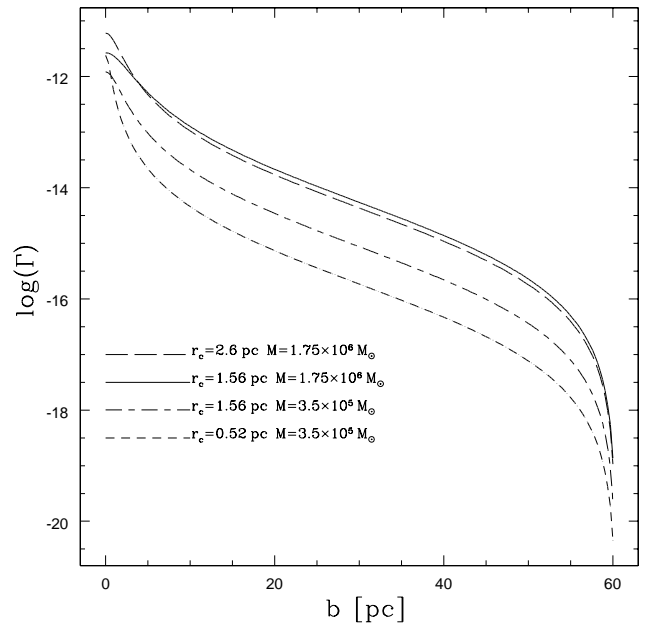**Fig. 10.** The microlensing event rate for the four different King models as described within the text.

Fig. 9. The optical depth for the four different King models as described within the text.

We then applied these results to study microlensing by globular clusters towards the galactic center, where locally the optical depth can be dominated by dark matter inside clusters. However, since globular clusters are very localized objects, the expected number of events as obtained by these scaling arguments is small. A larger event rate is expected, if the average MACHO mass inside the cluster is well below one solar mass, the total amount of dark matter is larger than $3.5 \times 10^5 M_\odot$ or the density of observable stars behind the cluster is significantly higher than the assumed value of 50 stars per $(1.2\,\mathrm{pc})^2$. Indeed, analysing the event distribution around the three clusters inside the observation fields of MACHO and OGLE, we find an increase of the microlensing event rate by at least a factor of about 2, as compared to that expected for MACHOs located in the disk and the bulge. This increase suggests the presence of a substantial amount of dark matter in form of light objects such as brown dwarfs.

Given this promising preliminary results it is important to systematically analyse future lensing data as a function of the position around the mentioned globular clusters. In fact, having few more events at disposal will already be very helpful to draw more firm conclusions and get better limits on the content of dark matter in globular clusters.

In addition, we propose to favour observation fields around globular clusters for future campaigns. In particular NGC 6553 is a very promising candidate for lensing by dark objects in globular clusters, since its luminosity is high and also its distance is such that the tidal radius

of the cluster corresponds to a relatively large angular size. Moreover, it would be important to have more precise knowledge of v_d, which is at present one of the main sources of uncertainty.

References

Alard C., Guibert J., 1997, A&A **326**, 1.

Alcock C., Akerlof C.W., Allsman R.A. et al., 1993, Nat **365**, 621.

Alcock C., Allsman R.A., Alves D. et al., 1997a, ApJ **479**, 119.

Alcock C., Allsman R.A., Alves D. et al., 1997b, ApJ **486**, 697

Alcock C., Allsman R.A., Alves D. et al., 1997c, astro-ph 9708190

Auburg E., Bareyre P., Bréhin S. et al., 1993, Nat **365**, 623.

Binney J., Tremaine S., *Galactic Dynamics*, (Princeton University Press, 1987).

De Rújula A., Jetzer Ph., Massó E., 1991, MNRAS **250**, 348.

De Rújula A., Jetzer Ph., Massó E., 1992, A&A **254**, 99.

Gould A., 1997, astro-ph 9703050.

Griest K., Alcock Ch., Axelrod T.S. et al., 1991, ApJ **372**, L79

Gunn J., Griffin R., 1979, AJ **84**, 752

Gyuk G., Holder G.P., 1997, astro-ph 9710251

Harris W.E., 1996, AJ **112**, 1487

Heggie D.C., Hut P., 1996, *Dark matter in globular clusters*, Int. Astron. Union Symp. No. 174, p. 303-312

Hesser J.E, Harris W.E., Vandenberg D.A. et al, 1987, PASP **99**, 739

Jetzer Ph., 1991, *Atti del Colloquio di Matematica*, CERFIM (Locarno) **7**, 259.

Jetzer Ph., 1994, ApJ **432**, L43.

Jetzer Ph., Proceedings of the Workshop on Gravitational Lensing, eds. De Ritis et al. (Naples, October 1997), to appear

Jetzer Ph., Massó E., 1994, Phys. Lett., **B 323**, 347

King I., 1962, AJ **67**, 471

King I., 1966, AJ **71**, 64

Lang K., *Astrophysical Data: Planets and Stars*, (Springer Verlag, 1992)

Meylan G., 1989, A&A **214**, 106

Paczyński B., 1986, ApJ **304**, 1.

Paczyński B., 1994, Acta Astronomica **44**, 235.

Palanque-Delabrouille N., Afonso C., Albert J.N. et al., 1998, A&A **332**, 1

Rhoads J.E., Malhotra S., 1998, ApJ **495**, L55

Taillet R., Longaretti P.Y., Salati P., 1995, Astroparticle Physics **4**, 87

Taillet R., Salati P., Longaretti P.Y., 1996, ApJ **461**, 104

Udalski A., Szymański M., Stanek K.Z. et al., 1994, Acta Astronomica **44**, 165.

Udalski A., Kubiak M., Szymański M., 1997, astro-ph 9710091

Wandeler U., 1995, Diploma Thesis, University of Zürich, ZU-TH 23/95